Assessment of Radiometer Calibration With GPS Radio Occultation for the MiRaTA CubeSat Mission

Anne D. Marinan, Kerri L. Cahoy, *Member, IEEE*, Rebecca L. Bishop, Susan Seto Lui, James R. Bardeen, Tamitha Mulligan, William J. Blackwell, *Senior Member, IEEE*, Robert Vincent Leslie, Idahosa A. Osaretin, *Member, IEEE*, and Michael Shields

***Abstract*—The microwave radiometer technology acceleration (MiRaTA) is a 3U CubeSat mission sponsored by the NASA Earth Science Technology Office. The science payload on MiRaTA consists of a triband microwave radiometer and global positioning system (GPS) radio occultation (GPSRO) sensor. The microwave radiometer takes measurements of all-weather temperature (V-band, 50–57 GHz), water vapor (G-band, 175–191 GHz), and cloud ice (G-band, 205 GHz) to provide observations used to improve weather forecasting. The Aerospace Corporation's GPSRO experiment, called the compact total electron content and atmospheric GPS sensor (CTAGS), measures profiles of temperature and pressure in the upper troposphere/lower stratosphere (∼20 km) and electron density in the ionosphere (over 100 km). The MiRaTA mission will validate new technologies in both passive microwave radiometry and GPSRO: 1) new ultracompact and low-power technology for multichannel and multiband passive microwave radiometers, 2) the application of a commercial off-the-shelf GPS receiver and custom patch antenna array technology to obtain neutral atmospheric GPSRO retrieval from a nanosatellite, and 3) a new approach to space-borne microwave radiometer calibration using adjacent GPSRO measurements. In this paper, we focus on objective 3, developing operational models to meet a mission goal of 100 concurrent radiometer and GPSRO measurements, and estimating the temperature measurement precision for the CTAGS instrument based on thermal noise Based on an analysis of thermal noise of the CTAGS instrument, the expected temperature retrieval precision is between 0.17 and 1.4 K, which supports the improvement of radiometric calibration to 0.25 K.**

***Index Terms*—Calibration, microwave radiometry, radio propagation, remote sensing, space technology.**

Manuscript received October 1, 2015; revised January 26, 2016, May 9, 2016, and July 2, 2016; accepted July 23, 2016. Date of publication October 24, 2016; date of current version December 1, 2016. This work was supported by NASA under Grants NNX14AC75G and NNX14AL95G. *(Corresponding author: Anne D. Marinan.)*

A. D. Marinan was with the Aeronautics and Astronautics Department, Massachusetts Institute of Technology, Cambridge, MA 02139 USA. She is now with the Jet Propulsion Laboratory, Pasadena, CA 91109 USA (e-mail: anne.d.marinan@jpl.nasa.gov).

K. L. Cahoy is with the Aeronautics and Astronautics Department and Earth Atmospheric and Planetary Sciences Department, Massachusetts Institute of Technology, Cambridge, MA 02139 USA (e-mail: kcahoy@mit.edu).

R. L. Bishop, S. S. Lui, J. R. Bardeen, and T. Mulligan are with The Aerospace Corporation, El Segundo, CA 90245-4691 USA (e-mail: Rebecca.L.Bishop@aero.org; susan.s.lui@aero.org; james.r.bardeen@aero.org; Tamitha.M.Skov@aero.org).

W. J. Blackwell, R. V. Leslie, I. A. Osaretin, and M. Shields are with the MIT Lincoln Laboratory, Lexington, MA 02420-9185 USA (e-mail: wjb@ll.mit.edu; lesliev@LL.mit.edu; idahosa.osaretin@ll.mit.edu; shields@ll.mit.edu).

Color versions of one or more of the figures in this paper are available online at http://ieeexplore.ieee.org.

Digital Object Identifier 10.1109/JSTARS.2016.2598798

I. Introduction

TRADITIONAL weather satellites, such as the defense meteorological satellite program [1] and geostationary operational environmental satellite [2], are large monolithic high-value systems with complex scientific payloads that provide critical observations used for forecasting and monitoring. Such satellite missions typically have extensive development cycles and conservative risk postures. Recently, the design and architectures of remote sensing spacecraft, including weather satellites, have experienced a paradigm shift toward small satellites (<500 kg) with the miniaturization of instrumentation and increase in availability of launch opportunities. There has particularly been an increase in the development of "nanosatellites" for weather sensing [3]. This paper focuses on passive microwave radiometers and global positioning system radio occultation (GPSRO) instruments. One of the challenges in implementing instruments, such as passive microwave radiometers on a nanosatellite platform, is instrument calibration, which is typically done on larger satellites through the use of large stable internal hot and cold targets.

This paper describes the operational approach for obtaining GPSRO measurements within the same atmospheric volume and altitude range necessary for calibrating a colocated radiometer measurement, as well as the approach for obtaining the resulting temperature profile data products. The goal of this paper is to develop methods and models with which we can quantify the expected science yield of the microwave radiometer technology advancement (MiRaTA) mission and estimate the quality of the retrieved GPSRO temperature profile to be used to calibrate the radiometer. Section II goes into more detail on the MiRaTA mission, radiometer payload, and CTAGS sensor and calls out science objectives and performance requirements for each. Section III explains the simulation and results for an analysis of the frequency of occurrence and locations (latitude, longitude, and tangential height) of GPSRO observation opportunities. We are particularly interested in GPSRO that overlap with the field of view (FOV) of the radiometer to generate colocated measurements to facilitate radiometer calibration. Section IV explains the overall architecture and preliminary results for determining temperature measurement precision from GPSRO measurements on MiRaTA. We determine the expected temperature precision using predicted instrument error values from GPSRO subsystem hardware simulations and compare those results to precision levels necessary to obtain state-of-the-art (and better) absolute calibration accuracy for a microwave

radiometer. In simulations investigating the utility of hosting both the radiometer and GPSRO on a nanosatellite, Blackwell *et al*. showed that absolute calibration accuracy down to 0.25 K is achievable for temperature sounding channels in this band for a total-power radiometer using a weakly coupled noise diode for frequent calibration and proximal GPSRO measurements (assuming 0.3–0.4 K temperature error) for infrequent (approximately daily) calibration [4]. Future work and a follow-on study are required to assess the expected performance of this mission using functional and environmental test data from the instrument in flight configuration.

A. CubeSats

The term "nanosatellite" is applied to satellites that are $<$10 kg; a mass that is small enough to be easily accommodated as an auxiliary payload on launch vehicles. A CubeSat is a standardized form of nanosatellite. The CubeSat specification document developed by the California Polytechnic State University in 2000 [5] defines a CubeSat unit, or a "U" as the volume restriction of a cube with 10 cm on a side and mass of 1.33 kg per U. The widespread adoption of the CubeSat standard has resulted in a proliferation of commercial off-the-shelf (COTS) components "suitable" for use in space, including miniaturized power and communications systems as well as miniaturized attitude determination and control systems that take advantage of advances in microelectromechanical systems. The CubeSat units can be stacked or combined in a modular fashion, can be packed into single or multiple CubeSat deployers, and manifest on commercial or government launches to low Earth orbit; the National Aeronautics and Space Administration (NASA) maintains a CubeSat launch initiative program to increase launch availability to researchers.

CubeSat capabilities continue to improve [6], and there is considerable momentum to transition from scientific and academic proof-of-concept missions into dedicated observation missions that generate valuable operational data products. MIT and MIT Lincoln Laboratory have collaborated on two consecutive CubeSat efforts with the goal of advancing several technologies. This paper focuses on the MiRaTA mission, which is a NASA ESTO-funded program whose goal is to increase the technology readiness level of miniaturized weather sensing technologies [7]. MiRaTA will demonstrate a new and different approach to radiometer calibration by utilizing tropospheric temperature measurements obtained by an onboard GPSRO sensor. This paper describes the operational approach for obtaining GPSRO measurements within the same atmospheric volume and altitude range necessary for calibrating a co-located radiometer measurement, as well as the approach for obtaining the resulting temperature profile data products. The goal of this paper is to develop methods and models with which we can quantify the expected science yield of the MiRaTA mission and estimate the quality of the retrieved GPSRO temperature profile to be used to calibrate the radiometer.

B. Passive Microwave Radiometry

Microwave radiometry is a field of remote sensing concerned with measuring the radiation from the atmosphere at microwave wavelengths. Microwave radiometers on orbit collect thermal radiation emitted from molecules in the Earth's atmosphere. An antenna receives the signal and then supporting electronics detect and amplify this radiation within a certain frequency band. The magnitude of the received signal is related to the temperature of the molecules in the atmosphere. Radiometric observations can be used to estimate many important atmospheric parameters and characteristics, including temperature and water vapor profiles, which can inform meteorological modeling [8]. Atmospheric constituents have different absorption spectra, and sampling at different frequencies permits different depths of the atmosphere to be probed; for example, molecular oxygen lines are often used for determining temperature distribution [9].

The current state of the art for weather sensing satellites with microwave radiometers includes instruments like the advanced technology microwave sounder (ATMS) [10], the advanced microwave sounder unit (AMSU) [11], and the microwave humidity sounder [12]. These instruments are over 50 kg in mass, consume tens of watts of power, and are able to sample across multiple bands and tens of channels. Typically the antennas rotate in order to view the observational target (e.g., Earth), cold space, and an internal blackbody calibration source. The instrument uses the cold and hot targets for internal calibration that allows for measurement accuracy to sub-K levels [13]. As the current fleet of satellites ages, and with the goal of improved spatial and temporal weather measurements [14], recent research has focused on developing miniaturized microwave radiometers to fly on constellations of small satellites. CubeSat missions, such as PolarCube [15], the Microsized Microwave Atmospheric Satellite (MicroMAS) [16], Radiometer Acceleration CubeSat Experiment (RACE) [17], Radiometer Assessment using Vertically Aligned Nanotubes [18], IceCube [19], and the Microwave Radiometer Technology Acceleration (MiRaTA) [7] have housed 1U (10 cm $\times$ 10 cm $\times$ 10 cm) sized radiometers. Future missions are planned (e.g., EON [20]) for even more capable radiometer payloads on larger CubeSats.

One of the main challenges in shrinking passive radiometer systems onto a CubeSat-sized platform is maintaining consistent calibration. The internal calibration targets on instruments such as AMSU and ATMS are very stable, but they cannot be easily implemented on a 10 cm $\times$ 10 cm $\times$ 10 cm CubeSat-sized platform due to volume constraints and challenges related to thermal gradients and stray radiation containment. Instead, one common approach is to use a noise diode to inject known noise in the receiver module. Internal matched loads can also be used at select frequencies. Fig. 1 shows how these types of calibration methods are implemented on the MiRaTA radiometer (further described in Section II-B).

Other CubeSat missions have used or plan to use a similar noise injection method for on-orbit calibration. The MicroMAS, a precursor to the MiRaTA mission also developed by the MIT Lincoln Laboratory and the MIT Space Systems Laboratory, featured a scanner assembly to spin the payload at $\sim$40 r/min in order to allow the radiometer to scan across the Earth and cold space. The $\sim$3 K of deep space and an internal noise diode served as the cold and warm calibration points, respectively. The satellite experienced a loss of communication shortly after power-on, and on-orbit calibration information was not

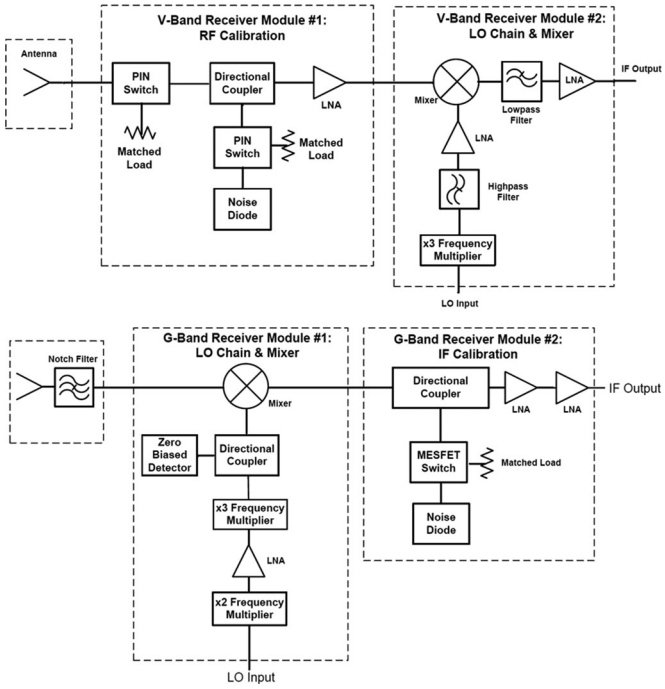

Fig. 1. Diagram of MiRaTA radiometer internal electronics. Top: The V-band receiver modules include an internal matched load as well as a noise diode. Bottom: The G-band receiver modules include a noise diode.

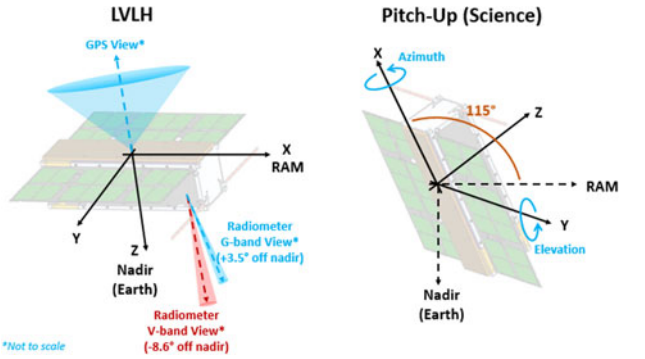

Fig. 2. MiRaTA axes and orientation nomenclature. Left: LVLH orientation. Right: Pitched-up orientation to achieve GPSRO with assumed 115° pitch-up angle.

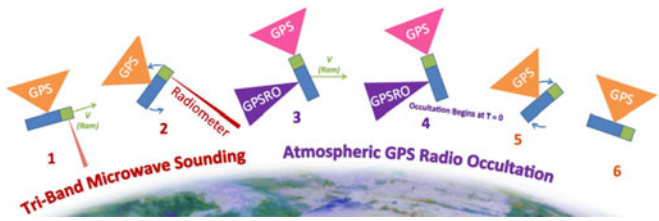

Fig. 3. MiRaTA CubeSat primary mission validation concept of operations pitch-up Maneuver [4].

collected. MicroMAS-2, scheduled for launch in early 2017, is a reflight of the MicroMAS mission and will host a four-band radiometer [20] RACE, developed by JPL, incorporated a noise diode coupled to an low-noise amplifier (LNA) as well as used periodic views of deep space for its internal calibration [17], but RACE experienced a launch failure in 2014. IceCube [19] and PolarCube [15] also inject noise using an internal diode.

Switches for internally matched loads can be lossy (or unavailable), and the long-term stability of noise diodes is variable. Noise diode drift can range from 0.5% to 3%, which is not currently as low as the larger heritage calibration targets [13]. Additional calibration methods are needed on these systems to enable absolute calibration accuracy better than 1 K over mission lifetimes [4]. One goal of MiRaTA is to provide a way to calibrate the noise diode using GPSRO profiles, which will be described further in Section III.

II. MiRaTA Mission and Payloads

A. Mission Operations

The primary science payload on MiRaTA is a triband microwave radiometer. It is important to calibrate such instruments, ideally with a National Institutes of Standards and Technology-traceable source. For MiRaTA, the mission requirements stipulate that the radiometer measurement accuracy shall be no worse than 1.5 and 2.0 K at V band and G band, respectively, which is roughly double the requirements for the state-of-the-art ATMS instrument [21]. Historically, satellites with microwave radiometers have included relatively large internal calibration targets, which are problematic for a CubeSat due to tight volume and mass restrictions. The plan for MiRaTA is to calibrate its radiometer using cold space and a noise diode, with characterization of the noise diode drift calculated based on radiometer measurements and GPSRO measurements sampled from overlapping volumes of atmosphere.

MiRaTA will be launched into a sun-synchronous elliptical (440 × 811 km) orbit on NASA's Educational Launch of Nanosatellites (ELaNa-14) mission. Because of the configuration of the sensors on the spacecraft as well as navigational and power subsystem requirements, MiRaTA will use two operational modes. In the first or "nominal" mode, the radiometer is pointed nadir and the CTAGS antenna is directed zenith. This configuration allows the satellite to maintain a low drag profile and adjust the orientation of the solar panels with respect to the sun for optimal power draw. CTAGS provides position information as it includes a global positioning system (GPS) receiver. A second operational mode, "pitch-up" mode, is required to enable the CTAGS calibration measurements. Fig. 2 shows the MiRaTA spacecraft with axes defined for the orientations of the local vertical local horizontal (LVLH) and pitched-up spacecraft orientations.

The satellite performs a periodic "pitch-up" science maneuver, shown in Fig. 3. For each science maneuver, the satellite starts in a LVLH stabilized orientation with the radiometer pointed toward Earth and the GPS antenna toward deep space. The radiometer is powered on and the satellite pitches up to allow the radiometer to scan the Earth's limb and holds its attitude between 113° and 118° from LVLH (with the CTAGS antenna boresight at or slightly below the limb). To estimate the performance and spacecraft resource utilization, we developed a

simulation of the transition from normal mode to pitch-up mode. The simulation assumes MiRaTA reaches a final pitch-up angle of 115° regardless of its altitude (tailoring the simulation for the actual pitch-up profile given the elliptical orbit and constraints of the onboard attitude control system is an item for future work). This allows the CTAGS antenna to point toward the limb of the earth, and as the satellite flies, it collects occulted GPS signals from nearly the same volume of atmosphere as that scanned by the radiometer.

The GPSRO and radiometer measurements need to overlap at a minimum tangential height of 18–22 km within 100 km (horizontal) of the radiometer boresight. The desired overall precision of CTAGS temperature measurements is less than 1.5 K (goal of 0.5 K). Section IV contains a description of our planned approach to calculate retrieved temperature precision for CTAGS.

B. MiRaTA Radiometer

MiRaTA supports a triband radiometer sampling at V-band (50–57 GHz) and G-band (175–191, 205 GHz). The half-power beamwidth (HPBW) of the radiometer at V-band is 5.6° and G-band is 1.7°. The G-band beam is about 3.5° off-axis from spacecraft z-axis, and the V-band beam boresight is offset by 8.6° in the other direction (see Fig. 2). The V-band nadir footprint ranges from 45 to 84 km through the orbit. The radiometer is expected to achieve absolute radiometric accuracy of 1.5 K at V-band and 2.0 K at G-band [7], while radiometric precision at V-band is expected to be better than 0.1 K NEdT (noise equivalent delta temperature), and at G-band, better than 0.3 K NEdT. The GPSRO measurements are primarily used for V-band calibration. In simulations investigating the utility of hosting both the radiometer and GPSRO on the bus, Blackwell *et al.* showed that absolute calibration accuracy down to 0.25 K is achievable for temperature sounding channels in this band for a total-power radiometer using a weakly coupled noise diode for frequent calibration and proximal GPSRO measurements (assuming 0.3–0.4-K temperature error) for infrequent (approximately daily) calibration [4].

C. MiRaTA GPSRO Sensor

GPSRO is a measurement technique that utilizes a GPS receiver on a satellite in LEO to observe changes in GPS signals as the transmitting satellite is occulted by the Earth. These electromagnetic signals interact with the Earth's atmosphere from the LEO orbit altitude to the surface resulting in changes in the phase and pseudo range. These changes can then be used to extract temperature profiles in the lower atmosphere and plasma density in the ionosphere [22].

Beginning in 1995, GPSRO sensors consisting of a GNSS/GPS receiver, RF front-end electronics, and single patch or antenna arrays have successfully flown and obtained both ionospheric and tropospheric observations. The majority of the receivers were designed and built by the Jet Propulsion Laboratory—TurboRogue (GPS-MET, PICOSat-9), BlackJack (CHAMP, COSMIC/FORMOSAT-3, C/NOFS), and TriG (COSMIC-2)—and weigh up to 30 kg and draw up to 50 W of power [23]. At tangential heights between 10 and 20 km, closed-loop systems, such as GPS-MET and CHAMP, have demonstrated temperature precision down to 0.5–1.0 K [24], [25]. While very capable, their size, weight, and power requirements prevent their use on CubeSat or other nanosatellites.

Nanosatellites have carried GPS receivers for position and navigation data since 2000 [26] but have only recently been adapted to obtain occultation measurements. There has been significant progress in the development, space qualification, and flight of miniaturized GPSRO sensors focusing on the ionosphere. In 2008, the first COTS sensor for GPSRO was flown on a nanosatellite, but unfortunately due to spacecraft issues, no occultation products were obtained [27]. The first successful demonstration of a GPSRO sensor on a nanosatellite occurred in 2011 with the launch of the PSSCT-2 mission [28]. PSSCT-2 contained the compact total electron content sensor (CTECS) designed and built by The Aerospace Corporation, a predecessor of the MiRaTA CTAGS payload. CTECS was also flown as a part of the SENSE mission. CTECS successfully produced ionospheric TEC profiles from both missions [28]. Other CubeSat-sized sensors flown or under development include the PolaRx2, FOTON, and Pyxis [29].

The CTEC and Atmospheric GPS Sensor (CTAGS) consists of a COTS GPS dual-frequency (L1 at 1575.42 MHz and L2 at 1227.60 MHz) receiver (NovAtel OEM628) with custom firmware modifications, a custom three-element dual-frequency patch antenna array, and LNA/RF front end. The CTAGS antenna is mounted on the MiRaTA spacecraft on the opposite face as the radiometer FOV (in "nominal" mode, the radiometer faces nadir and the CTAGS antenna faces zenith providing navigation data). The MiRaTA CTAGS payload is designed to accept customizable commands. Specifically, it allows differing sampling rates depending on the elevation and azimuth of the GPS constellation satellite location relative to MiRaTA. In the nominal operating mode, CTAGS samples at 0.1 Hz for nonoculting satellites and 1 Hz for occulting. In the occultation mode, CTAGS samples at 50 Hz for occulting satellites and for a single above horizon reference satellite. The use of a dual-frequency receiver supports straightforward removal of clock errors and the effects of the ionosphere from troposphere and mesosphere observations.

Measurements made by the radiometer will be compared to radio occultation measurements of the nearly same volume of atmosphere. For this mission, CTAGS provides exclusively "setting" or "ingress" occultations providing a solid lock on signals as they pass through the mesosphere and troposphere. "Rising" or "egress" occulting signals may not be locked on until they are well above the troposphere/mesosphere.

III. Radiometer Calibration Process

Blackwell *et al.* [4] related GPS-derived refractivity error (nominally 0.002 fractional error for altitudes between 10 and 20 km) to radiometer brightness temperature calibration error, using 0.002 fractional refractivity error to produce an absolute radiometer calibration accuracy of 0.25 K. The calibration method presented in [4] takes place in two parts. First, a quadratic relationship between the GPSRO refractivity

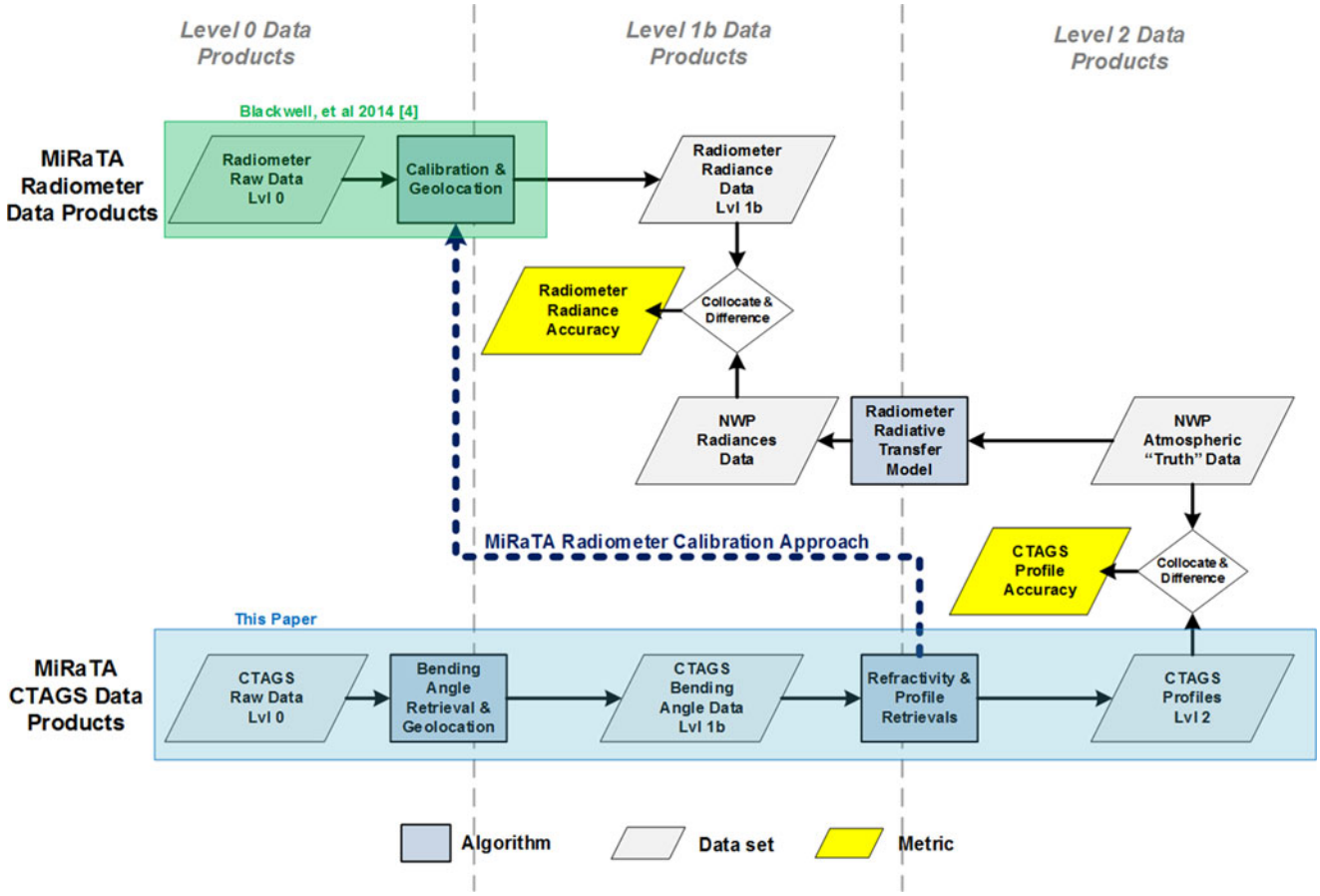

Fig. 4. Ground processing and validation flow for the MiRaTA mission data products (blue highlight box indicates contributions from this paper).

profile versus tangent height *N(h)* and radiometer brightness temperatures at a particular observing angle and frequency band of interest $T_B(\theta, f)$ is derived. Second, the radiometer gain *g* (in Kelvin/count, where "count" is the output of a 16-bit A/D converter) is chosen to minimize the residual between the calibrated and GPSRO-derived brightness temperature. Errors due to the quadratic estimation are treated in a weighted least squares sense.

Fig. 4 shows the science data validation process for the MiRaTA mission with the contributions from this paper (CTAGS data products) called out in the light blue box. The refractivity from the GPSRO measurements are used to calibrate the radiometer as described in [4]. Truth data (middle line) are obtained from numerical weather prediction (NWP) model outputs (e.g., ECMWF) and radiosonde measurements and are used to validate the radiometer data. The intrinsic GPSRO retrieval performance is also assessed through comparison against the NWP and radiosonde data to evaluate the fundamental utility (accuracy and precision) of the GPSRO temperature retrievals.

In this paper, we characterize the precision associated with the GPSRO retrieved profiles. While the radiometer calibration process uses GPSRO-derived refractivity profiles in its calculations, Kursinski [22] relates GPS refractivity error to temperature profile retrieval error, showing that a fractional refractivity error of 0.002 corresponds to a temperature error of approximately 0.5 K for altitudes between 10 and 20 km. We, therefore, use 0.5-K GPSRO temperature error as the threshold requirement to achieve the 0.25-K brightness temperature error reported in Blackwell *et al*. This paper presents an analysis of the MiRaTA GPSRO retrieved temperature and compares with the 0.5-K requirement.

A. GPSRO and Radiometer Overlap

Understanding and predicting the occurrence of coincident occultations is critical to mission operations related to scheduling the calibration maneuver. The atmosphere observed by the radiometer and CTAGS should overlap as much as possible in order to accomplish the calibration objectives of the MiRaTA mission [4]. The design orbit is elliptical, so the timing of each science maneuver will have to take into account the radiometer sampling location (making sure it scans the limb at the correct latitude and longitude) and the amount of time it will take the satellite to propagate to the location where it can capture the occultation. It takes less than a minute for the GPS satellite to set once line of sight to the GPS satellite from the perspective of MiRaTA has reached a tangential height of 25 km.

In order to calibrate the radiometer by comparing refractivity profiles from both GPSRO and radiometer measurements, measurements from the CTAGS and radiometer instrument must overlap spatially and temporally. This minimizes errors due to

TABLE I
CHANNEL PARAMETERS FOR THE MIRATA RADIOMETER [4]

Channel ID	Type	Center Frequency (GHz)	Bandwidth (MHz)	Weighting Function Peak Height (km)
V1	Single-Side Band	50.30	180	0
V2		51.76	400	0
V3		52.80	400	2
V4		53.50	600	5
V5		54.40	400	8
V6		54.94	400	11
V7		55.50	330	13
V8		56.65	600	18
G1	Double-Side Band	183.31 ± 1	500	7
G2		183.31 ± 3	1000	4
G3		183.31 ± 5	2000	2
G4		204.8	2000	1

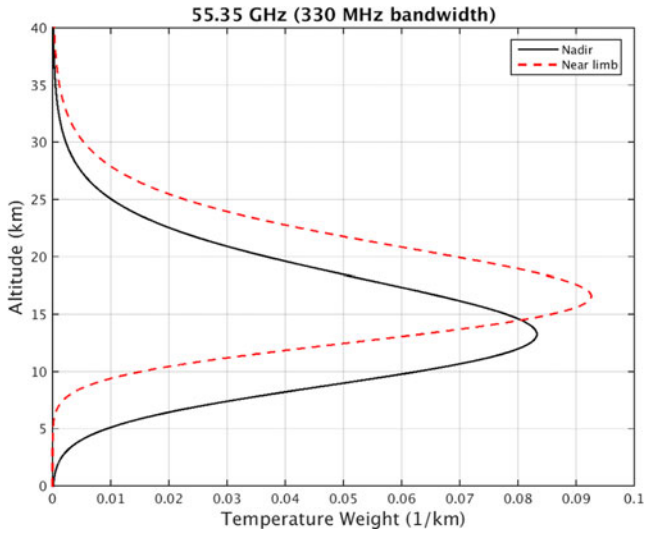

Fig. 5. When limb facing, the radiometer weighting function is ~3.5 km higher than when the radiometer is nadir facing.

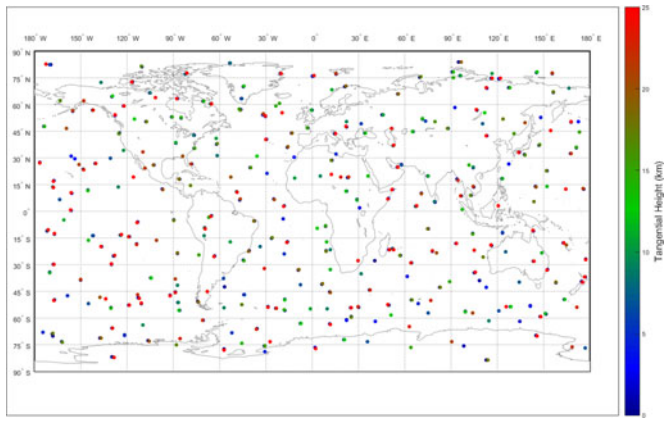

Fig. 6. Tangential height (<25 km) as a function of latitude and longitude for all visible setting GPS satellites over one day.

mismatched conditions during each measurement [30]. Based on the MiRaTA orbit geometry, measurements from CTAGS and the radiometer will overlap within a 10–15-min window, and we specify that CTAGS measurements valid for calibration must fall within 100 km of the radiometer FOV. Over these temporal and spatial scales, we can assume the upper tropospheric/lower stratospheric temperature is invariant [31]. This is consistent with collocation in past efforts to calibrate ATMS using GPSRO measurements [32], though it is also possible to use GPSRO-calibrated radiometer measurements to calibrate other radiometer measurements where collocated GPSRO data are not available [33].

In this simulation, which is focused on sounding overlapping atmospheric volumes and developing an approach for estimating GPSRO temperature profile precision, we are not concerned with radiometer signal-to-noise ratio (SNR), just the geometric "FOV." When the radiometer is pointed to the limb, depending on the spacecraft location in the elliptical orbit, the $\pm$100-km overlap range corresponds to an angle of about 2° as seen by the spacecraft. Thus, the radiometer receive "FOV" in the simulation (limb facing) is defined as 2° based on the 100-km overlap requirement, rather than the full V-band 5.6° HPBW. The radiometer "FOV" boresight is offset from the spacecraft z-axis by 8.6° so in order to compare CTAGS and radiometer temperature measurements; an occultation needs to occur when a GPS satellite passes through an azimuth window between 187.6° and 189.6° with respect to MiRaTA (see Fig. 2 for orientation convention).

The desired tangential height range for the overlapping radiometer and CTAGS calibration measurements is 18 to 22 km. This tangential height was chosen based on the weighting functions for each of the MiRaTA radiometer's 12 channels (see Table I). The weighting function is for a nadir-facing beam. When the radiometer faces the limb, the weighting function peak height will be a few kilometers higher as shown in Fig. 5. As described in Blackwell *et al.* [4, Fig. 2], a relationship between the GPSRO measurements and the radiometer brightness temperature as a function of scan angle is derived, and the brightness temperature distribution over the limb scan is then used to estimate the needed calibration parameters. Ideally, we would like to sample at lower altitudes with GPSRO, but this will depend on the ability of the CTAGS instrument to maintain lock on signals through the lower atmosphere. The derived relationship between GPSRO and radiometer brightness temperature in Blackwell *et al.* [4] added random refractivity noise to the calculated refractivity at a level commensurate with that reported by Kursinski [22] to model these issues.

Fig. 6 illustrates the expected latitude and longitude distributions of all possible GPS occultation opportunities with tangential heights under 25 km over a period of 24 h. The tangential heights are captured in the color bar (0- to 25-km scale). MiRaTA will see a daily average of 6 setting occultations that occur within the FOV of both the CTAGS antenna and the radiometer. Over three months, there are 520 occultations that fall within the azimuth and elevation viewing requirements and reach a tangential height of less than 25 km. The latitude and longitude positions of these events are depicted in Fig. 7 (which uses the same color scale as Fig. 6).

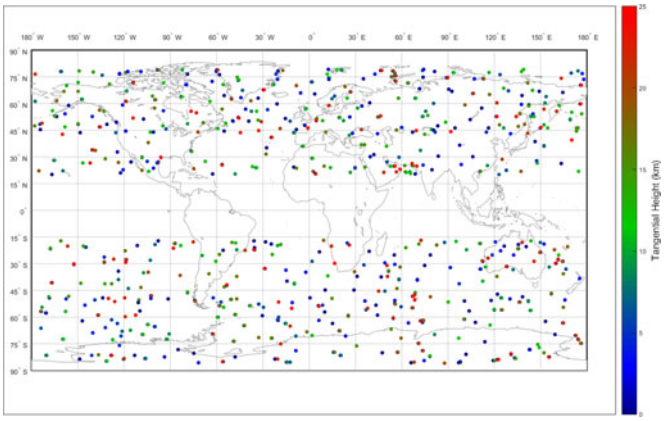

Fig. 7. Tangential height (<25 km) as a function of latitude and longitude for all visible setting GPS satellites within the radiometer FOV over three months.

This modeling effort will continue to be refined in the coming months to take into account atmospheric bending and calculating the exact overlap of the 3-D volume of atmosphere that the CTAGS and radiometer each measure (the simulation currently considers two dimensions, one dimension in azimuth with respect to the MiRaTA spacecraft, and one dimension with respect to tangent height line-of-sight to the GPS satellite). For the CTAGS measurements, this volume can be estimated using the geometry of the first Fresnel zone, which depends on the tangential height and the relative positions of the GPS satellite transmitter and MiRaTA receiver, and in the atmosphere on the ratio of $\mathrm{SNR_v}$ to $\mathrm{SNR_v^0}$ (1-s SNR in free space) [24]. We also plan to include a more detailed rendering of the radiometer sampling pattern and the sensitivity of the system to pointing and timing offsets in future model updates.

IV. Estimation of Temperature Retrieval

For this analysis, we follow the framework set by of Hajj *et al.* 2002 [24] to calculate bending angle precision based on the expected received $\mathrm{SNR_v}$ (voltage SNR ratio) at CTAGS. Fig. 8 illustrates the steps taken in this process.

Due to the similarities between the MiRaTA mission and the GPS-MET instrument (closed-loop receivers, similar SNR), we compare our results to the simulated performance of that mission. The numbers from the Kursinski analysis [22] were used as assumptions in the calculation of the impact of GPSRO measurements on the radiometer calibration accuracy in [4].

A. SNR Calculations and Assumptions

SNR calculations require an understanding to the link budget of the system. We start with the assumption that the CTAGS instrument is able to receive signals through the atmosphere with enough SNR to lock and track the transmitting GPS satellite through a complete occultation event (i.e., signals encounter solid Earth). A link budget calculation supports this assumption. The transmit power and gain are simulated using Analytical Graphics, Inc., System Tool Kit GPS transmitter models at L1 and L2 frequencies. The CTAGS antenna gain pattern was provided by The Aerospace Corporation during the design model phase for their custom array (maximum passive gain 9.7 dB at L1 and 9.4 dB at L2). The ideal pointing for the antenna is for the minimum elevation angle of observation (at or slightly below the limb of the Earth) to line up within the HPBW of the antenna boresight. For an elliptical orbit, the ideal pitch-up angle will vary with orbit altitude, but for the results in this study, the pitch-up angle is assumed to be a constant 115° (pointed directly at the limb at an altitude of 625-km orbit).

Noise parameters were either calculated or taken from component datasheets. The system noise temperature includes antenna noise (150 K assuming that the Earth will be in half of the antenna FOV), receiver noise figures, and interference from other GPS satellites in the FOV(assuming total 200 K). The Novatel OEM628 receiver that was modified for the CTAGS instrument is a COTS component, and as such, specific noise parameters are proprietary information. For now, we assume that the external LNA noise dominates the receiver noise. Future studies will incorporate noise figures as measured from open-air (and eventually on-orbit) tests of the integrated system. Atmospheric losses are currently based on the ITU-R P676-9 model up to 100 km [34]. Bending due to refraction is not included in the current model.

The Novatel receiver is sensitive to signals between 20 and 50 dB-Hz. We have not accounted for all losses, but with the conditions specified above there is enough margin (>20 dB) to expect that the signal can be received through the atmosphere down to the required temperature height based on similar calculations done for GPS-MET [22].

B. Calculating Bending Angle Error

The SNRv (V/V) of the received signal does ultimately impact temperature error. The Novatel receiver datasheet [35], lists a thermal phase noise mean square error of 0.5 mm for the L1 frequency, and 1 mm for L2, for a nominal sampling frequency of 20 Hz (0.05-s integration time). From the following relationship

$$\left\langle \delta\phi(\tau)^2 \right\rangle^{\frac{1}{2}} = \frac{\lambda}{2\pi}(2\mathrm{SNR}_0\tau)^{-\frac{1}{2}} \tag{1}$$

where $\langle \delta\phi^2 \rangle^{\frac{1}{2}}$ is the rms phase error (units of length), λ is the sampling frequency (L1 or L2), τ is the integration time, and SNR_0 (W/W) is the power SNR based on a 1-s integration time ($\mathrm{SNR}_0 = \mathrm{SNR}_{v_0}^2$, where SNR_{v_0} is the voltage SNR in a vacuum) (Hajj *et al.* [24]), we calculate that the 1-s L1 $\mathrm{SNR_v}$ of the receiver is 271 V/V (174 V/V for L2). The receiver on the CTAGS instrument has been reconfigured from its default to sample at 50 Hz, but for retrieval measurements, we assume that the integration time is the time it takes the signal to vertically travel a Fresnel diameter through the atmosphere. The Fresnel diameter will vary through the atmosphere as the signal is degraded. For the receiver SNR_{v_0} the average value for MiRaTA is 1.4 km. The average integration time for the MiRaTA orbit (440 km × 811 km) is 0.5 s, which corresponds to a 0.16-mm phase precision (0.32 mm for L2).

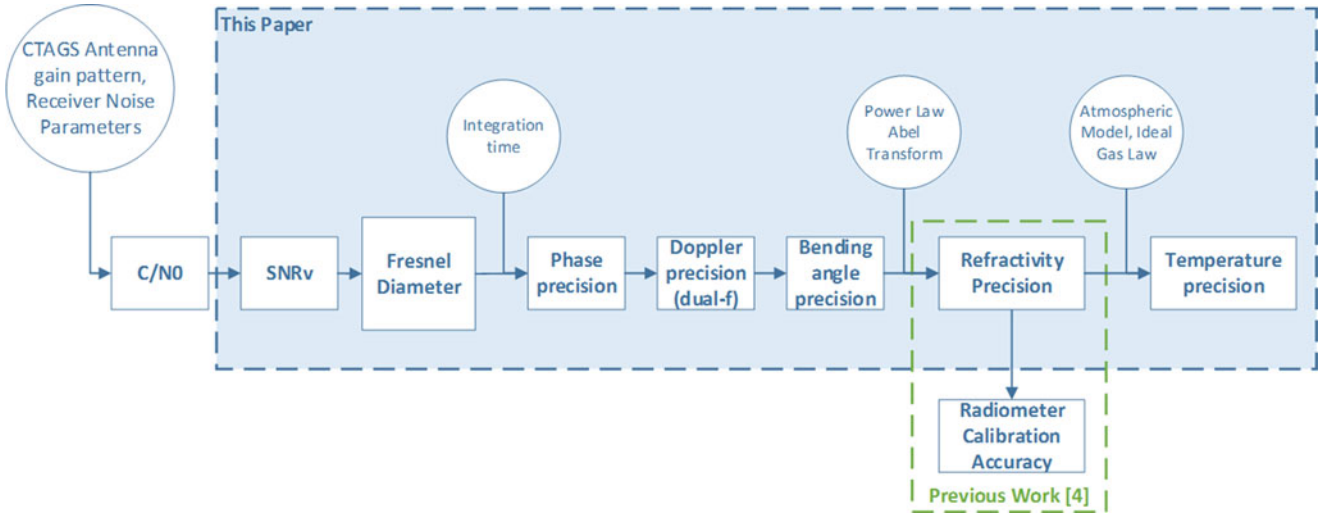

Fig 8. Process for estimating temperature precision for the MiRaTA GPSRO measurements based on the thermal phase noise. The focus of this paper is highlighted in the shaded box. Further studies will account for other sources of error.

Phase precision feeds into the Doppler noise and ultimately to bend angle precision through the following relationships (Hajj *et al.* [24]):

$$\sigma_{\text{Doppler}} = \frac{\sigma_\phi \sqrt{12}}{\Delta N^{3/2}} \tag{2}$$

$$\sigma_\alpha = \frac{\lambda \sigma_{\text{Doppler}}}{V_0} \tag{3}$$

$$\sigma^2_{\alpha_{\text{neut}}} = (2.54)^2 \sigma^2_{\alpha_1} + (1.54)^2 \sigma^2_{\alpha_2} \tag{4}$$

where Δ is the time between successive measurements (50-Hz sampling), N is the number of samples averaged over one measurement, which we calculate based on Δ and the time it takes for the signal to cross one Fresnel diameter, V_0 is the vertical speed of the signal tangent point through the atmosphere in m/s, and the phase error σ_ϕ is in units of cycles. Because we are sampling at two frequencies, we take the error from both L1 and L2 into account in (4) (Hajj *et al.* [24]). Fig. 9 shows the estimated bending angle error ($\sigma^2_{\alpha_{\text{neut}}}$) through the neutral atmosphere as a function of tangential height for the SNR_v values used above. In the next section, we describe how this calculated bending angle propagates to temperature precision

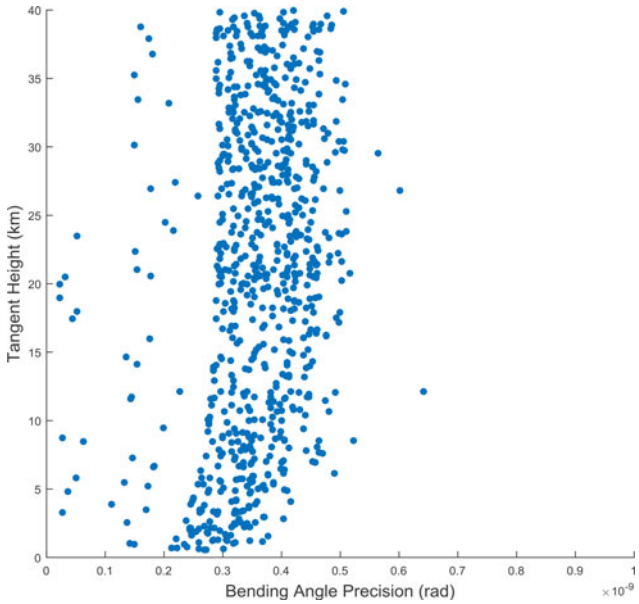

Fig. 9. Bending angle precision versus tangential height predicted for the thermal noise error contributions (does not include atmospheric conditions, clock noise, position/velocity errors, or multipath effects).

C. Temperature Retrieval Error

The Abel transform is applied to the bending angle to calculate refractivity, and then temperature can be derived using standard atmospheric temperature assumptions (for details, see [22]). Our approach to the Abel transform was to use a low-noise power law approximation of atmospheric refractivity [Hinson, pers. corr. 2010]. We assume a 1° bending at the surface [36] and a scale pressure height of 7.5 km [37]. Because the Abel transform of a power law function model input has an analytic solution, we can compare the analytic solution with numerical calculation to assess the contribution of the numerical calculation to the retrieval error. As shown in Fig. 10, the numerical error contribution from performing the transform on a representative Earth bending angle profile is negligible.

D. Error Propagation to Temperature Precision

The results from the bending angle error simulation represent the standard deviation of measured bending angle expected for the CTAGS instrument. We generate a Gaussian noise distribution with this standard deviation (0.3e−9 rad) and add it to a simulated vector of bending angles using the power-law approximation described in the previous section. Two vectors of bending angles versus atmospheric height are fed into the Abel transform simulation, one with added noise, and one without.

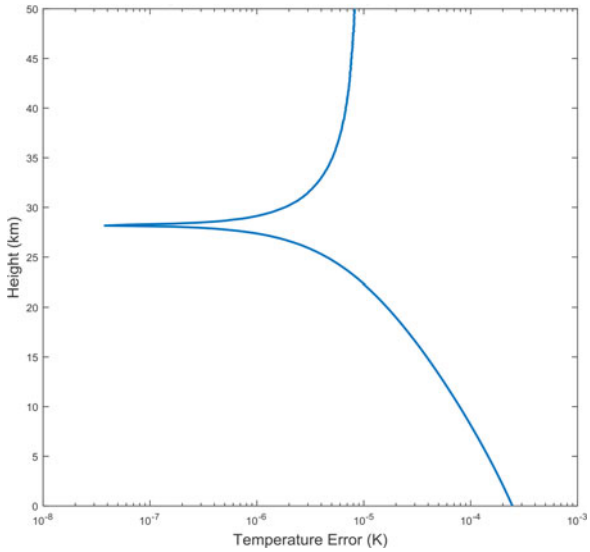

Fig. 10. Error in temperature calculations due to numerical approximations in performing the Abel transform. For a detailed treatment of the radio occultation mapping kernel, see Ahmad 1998 [38].

For this initial assessment, we do not yet take into account any bias or offset in these measurements. Fig. 11 shows the profile of the noise added to the power-law approximation of bending angle in the model. The temperature error that comes out of this (measured as the absolute difference between the results with and without the bending angle error) is between 0.1 and 1 K for the heights of interest.

The MiRaTA mission requires a 1.5-K temperature retrieval precision in the neutral atmosphere through GPSRO measurements with a goal of 0.5-K temperature precision. A 0.5-K temperature precision (goal) obtained from the CTAGS instrument would satisfy the conditions necessary to achieve a 0.25-K absolute accuracy in calibration of the radiometer (note: the requirement for state-of-the-art ATMS measurements is 0.75 K in V-band as shown in [19], and AMSU-A had a 1.5-K absolute calibration accuracy requirement [39]). The thermal noise error calculated in this simulation has a 95% confidence interval between 0.17 and 1.4 K. This thermal noise impact on temperature precision indicates that the CTAGS instrument will be able to meet its temperature retrieval requirements in support of radiometer calibration. At the lower end of this confidence interval, the instrument has comparable performance to missions such as GPS-MET, which saw a worst-case overall temperature error of 0.4 K (taking into account more than just thermal error) at the altitudes of interest for MiRaTA [22].

E. Other Sources of Error

The analysis presented so far has been only for the measurement error due to the thermal noise. Table II summarizes the effects of several other sources of error.

From the thermal error input, we can determine that the CTAGS expected thermal noise impact on the temperature precision at 20-km tangential height is on the same order as that calculated by Kursinski for the GPS-MET mission—0.17 K best case for CTAGS and ∼0.1 K for GPS-MET [22]. The other

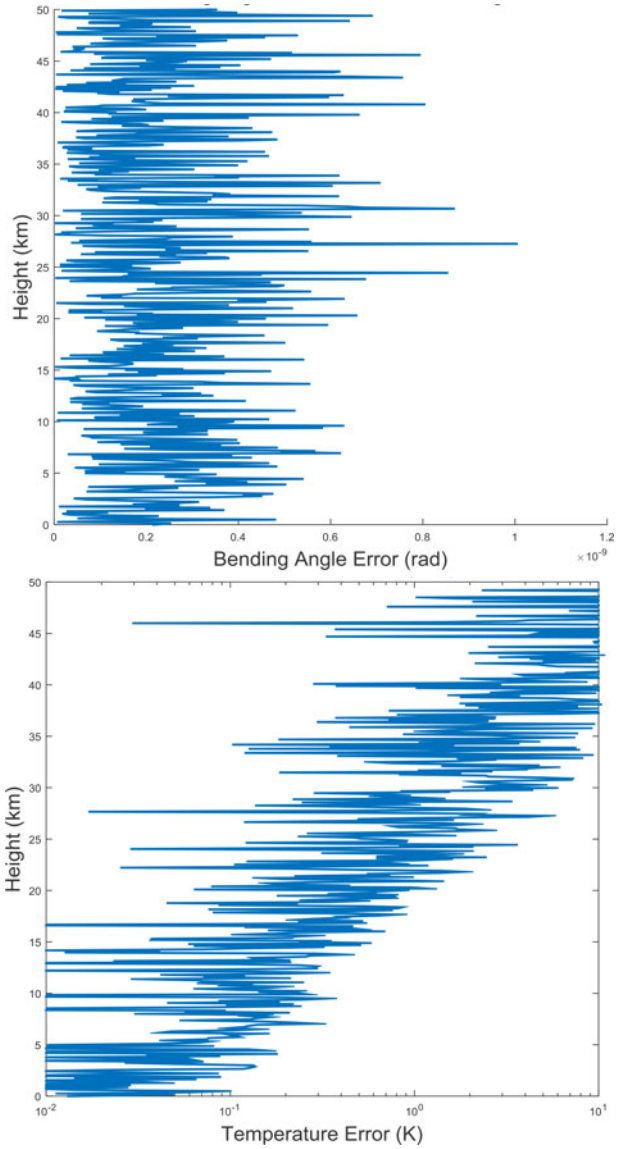

Fig. 11. (Top) Bending angle error input to the numerical Abel transform calculation. (Bottom) Corresponding retrieval temperature error. The error used for input was based on the thermal noise contributions and does not include atmospheric conditions, clock error, velocity/position errors, or multipath effects.

main sources of error, particularly local multipath, horizontal along-track errors, ionospheric effects, and Abel boundary, are important to characterize but are dependent on the environment and measurement conditions or the retrieval algorithm rather than on parameters specific to the instrument hardware itself.

V. Summary

The purpose of this study is to present the operational overview and scientific requirements for the MiRaTA mission to calibrate microwave radiometer measurements with GPSRO measurements. In order to accomplish the scientific goals, the system must perform neutral atmosphere temperature profile retrieval with precision <1.5 K at altitudes from 18 to 22 km and have an overlapping volume of observed atmosphere between the radiometer and GPSRO receiver.

TABLE II
TEMPERATURE ERROR FOR A VARIETY OF NOISE SOURCES BASED ON THE KURSINKSI STUDY OF GPS-MET FOR MIRATA'S ALTITUDE RANGE OF INTEREST [22]

Noise Source	Temperature Error (K)		
	10 km	20 km	30 km
Thermal error	0.03	0.1	0.4
Local multipath	0.07	0.2	0.5
Horizontal along track	0.3	0.2	0.2
Horizontal drift	0.1	<0.01	0.03
Ionosphere day, solar max	<0.01	0.2	0.7
Abel boundary, 5% Hφ	<0.01	<0.01	0.04
Abel boundary, 7% dα	0.04	0.2	0.7
Hydrostatic boundary	<0.01	<0.01	<0.01
H2O at 0 latitude, 0.5-km correlation length	<0.01	<0.01	<0.01
RSS Temperature Error	**0.6**	**0.4**	**1.1**

The conditions are: Thermal Error, 1-s SNR(W) = 5e4; local multipath, 10-mm rms Spread over 0.01 Hz; horizontal refractivity structure, along track from simulation and horizontal motion of ray path tangent point from tropospheric and stratospheric climatologies near 30°S for June–August; ionosphere error, daytime, solar maximum conditions; Abel boundary error, 7% in α, 5% in Hφ; hydrostatic boundary error, 5 K; tropospheric water vapor, 0° latitude with 8-km vertical correlation length.

We have modeled the CTAGS GPSRO experiment on MiRaTA and predict that over the course of three months, over 30 000 GPSRO observations can be made down to an altitude of less than 20 km. Of these, around 520 (6 per day) would at least partially overlap atmospheric volumes with the radiometer.

An initial estimation of the retrieved temperature precision showed that the MiRaTA payload should meet the requirements (1.5-K requirement, 0.5-K goal) for GPSRO temperature precision based on the thermal noise contribution of error. The calculated temperature precision based on thethermal noise is between 0.17 and 1.4 K, which is consistent with GPSRO performance on previously flown closed-loop systems. This analysis shows that from a hardware perspective, CTAGS performance should be able to contribute to an overall improvement of radiometer calibration state-of-the-art on a CubeSat platform. There are still several sources of error that have yet to be characterized, and future analysis will include measurements from hardware testing as well as use of the planned mission retrieval software in order to assess the end-to-end performance of the instrument. These results will better inform mission operations and the feasibility of meeting the science objectives.

ACKNOWLEDGMENT

The authors would like to thank the NASA Space Technology Research Fellowship Program, the Lincoln Scholars Program, and NOAA for support and the MiRaTA team for their insights and feedback. They would also like to thank T. Meehan, C. Ao, T. Mannucci, S. Asmar, and W. Williamson at JPL for their helpful feedback and suggestions, and D. Hinson at Stanford and SETI for use of his temperature retrieval method. At last, the authors would like to thank the journal's anonymous reviewers and service of its editorial staff for helpful suggestions and feedback.

REFERENCES

[1] NOAA. Defense meteorological satellite program (DMSP): Data archive, research, and products. 2013. [Online]. Available: http://ngdc.noaa.gov/eog/dmsp.html
[2] NOAA. NOAA's geostationary and polar-orbiting weather satellites. Mar. 5, 2014. [Online]. Available: http://noaasis.noaa.gov/NOAASIS/ml/genlsatl.html
[3] E. Buchen, *2014 Nano/Microsatellite Market Assessment*. Atlanta, GA, USA: SpaceWorks Enterprises, Inc., 2014.
[4] W. J. Blackwell *et al.*, "Radiometer calibration using collocated GPS radio occultation measurements," *IEEE Trans. Geosci. Remote Sens.*, vol. 52, no. 10, pp. 6423–6433, Oct. 2014.
[5] *CubeSat Design Specification, Rev. 13*, The CubeSat Program, California Polytechnic State University, San Luis Obispo, CA, USA, 2014.
[6] "Small spacecraft technology state of the art," National Aeronautics and Space Administration NASA/TP-2014-216648/Rev1, NASA Ames Research Center Mission Design Division Staff, Moffett Field, CA, USA, Jul. 2014.
[7] W. J. Blackwell *et al.*, "Microwave radiometer technology acceleration mission (MiRaTA): Advancing weather remote sensing with nanosatellites," presented at the *28th Annu. AIAA/USU Conf. Small Satellites*, Logan, UT, USA, 2014.
[8] K. Tomisayu, "Remote sensing of the earth by microwaves," *Proc. IEEE*, vol. 62, no. 1, pp. 86–92, Jan. 1974.
[9] E. Njoku, "Passive microwave remote sensing of the earth from space—A review," *Proc. IEEE*, vol. 70, no. 7, pp. 728–750, Jul. 1982.
[10] W. Blackwell, "Optimization and validation of ATMS climate data records," presented at the NOAA CDR Workshop, Mar. 3, 2011.
[11] AMSU-A. (2015, Sep.). Eumetsat: Monitoring Weather and Climate from Space. [Online]. Available: http://www.eumetsat.int/website/home/Satellites/CurrentSatellites/Metop/MetopDesign/AMSUA/index.html
[12] MHS. (2015, Sep.). Eumetsat: Monitoring Weather and Climate From Space. [Online]. Available: http://www.eumetsat.int/website/home/Satellites/CurrentSatellites/Metop/MetopDesign/MHS/index.html
[13] S. T. Brown, S. Desai, W. Lu, and A. Tanner, "On the long-term stability of microwave radiometers using noise diodes for calibration," *IEEE Trans. Geosci. Remote Sens.*, vol. 5, no. 7, pp. 1908–1920, Jul. 2007.
[14] *Polar-Orbiting Satellites: With Costs Increasing and Data Continuity at Risk, Improvements Needed in a Tri-Agency Decision Making*, United States Government Accountability Office, Washington, DC, USA, 2009.
[15] PolarCube: An advanced radiometer 3U CubeSat. (2015, Sep.). Colorado Space Grant Consortium. [Online]. Available: http://spacegrant.colorado.edu/allstar-projects/polarcube
[16] W. J. Blackwell *et al.*, "MicroMAS: First step towards a nanosatellite constellation for global storm observation," presented at the *27th Annu. AIAA/USU Conf. Small Satellites*, Logan, UT, USA, Aug. 2013.
[17] B. Lim. (2015, Sep.). Radiometer atmospheric CubeSat experiment (RACE). Jet Propulsion Laboratory, California Institute of Technology. [Online]. Available: http://phaeton.jpl.nasa.gov/external/projects/race.cfm
[18] H. J. Kramer. (2015, Sep.). RAVAN (radiometer assessment using vertically aligned nanotubes) mission. ESA. [Online]. Available: https://directory.eoportal.org/web/eoportal/satellite-missions/r/ravan
[19] D. L. Wu *et al.*, "IceCube: Spaceflight validation of an 874-GHz submillimeter wave radiometer for cloud ice remote sensing," presented at the *Earth Science Technol. Forum*, Leesburg, VA, USA, 2014.
[20] W. J. Blackwell and J. Pereira, "New small satellite capabilities for microwave atmospheric remote sensing: The earth observing nanosatellite-microwave (EON-MW)," presented at the *29th Annu. AIAA/USU Conf. Small Satellites*, Logan, UT, USA, Aug. 2015.
[21] C. Muth, P. S. Lee, J. C. Shiue, and W. A. Webb, "Advanced technology microwave sounder on NPOESS and NPP," in *Proc. IEEE Int. Symp. Geosci. Remote Sens.*, 2004, vol. 4, pp. 2454–2458.
[22] E. R. Kursinski, "Observing earth's atmosphere with radio occultation measurements using the global positioning system," *J. Geophys. Res.*, vol. 102, no. D19, pp. 23429–23465, 1997.
[23] O. Montenbruk, "GNSS receivers for space applications," in *ACES and Future GNSS-Based Earth Observation and Navigation*. Munchen, Germany: Tech. Univ. Munchen, 2008.
[24] G. A. Hajj, E. R. Kursinski, L. J. Romans, W. I. Bertiger, and S. S. Leroy, "A technical description of atmospheric sounding by GPS occultation," *J. Atmos. Solar-Terr. Phys.*, vol. 64, pp. 451–469, 2002.

[25] P. Staten and T. Reichler, "Apparent precision of GPS radio occultation temperatures," *Geophys. Res. Lett.*, vol. 36, no. L24806, 2009, doi: 10.1029/2009GL041046.
[26] Surrey Satellite Technology, Ltd. SNAP-1: The Mission. 2002. [Online]. Available: http://www.sstl.co.uk/Missions/SNAP-1-Launched-2000/SNAP-1/SNAP-1-The-Mission
[27] E. Kahr, L. Bradbury, P. G. O'Keefe, and S. Skone, "Design and operation of the GPS receiver onboard the CanX-2 nanosatellite," *Navigation*, vol. 60, pp. 143–156, 2013.
[28] R. L. Bishop *et al.*, "First results from the GPS compact total electron content sensor (CTECS) on the PSSCT-2 nanosat," presented at the *26th Annu. AIAA/USU Conf. Small Satellites*, Logan, UT, USA, 2012.
[29] G. Lightsey and T. Humphreys, "FOTON: A software-defined, compact, low-cost GPS radio occultation sensor," in *Proc. GEOScan Planning Workshop*, 2011, pp. 23–25.
[30] E. Fetzer *et al.*, "AIRS/AMSU/HSB validation," *IEEE Trans. Geosci. Remote Sens.*, vol. 41, no. 2, pp. 418–431, Feb. 2003.
[31] B. Tian, C. O. Ao, D. E. Waliser, E. J. Fetzer, A. J. Mannucci, and J. Teixeira, "Intraseasonal temperature variability in the upper troposphere and lower stratosphere from the GPS radio occultation measurements," *J. Geophys. Res.*, vol. 117, no. D15110, 2012, doi: 10.1029/2012JD017715.
[32] X. Zou, L. Lin, and F. Weng, "Absolute calibration of ATMS upper level temperature sounding channels using GPS RO observations," *IEEE Trans. Geosci. Remote Sens.*, vol. 52, no. 2, pp. 1397–1406, Feb. 2014.
[33] S.-P. Ho, M. Goldberg, Y.-H. Kuo, C.-Z. Zou, and W. Schreiner, "Calibration of temperature in the lower stratosphere from microwave measurements using COSMIC radio occultation data: Preliminary results," *Terr. Atmos. Ocean. Sci.*, vol. 20, no. 1, pp. 87–100, 2009.
[34] *Recommendation ITU-R P.676-10: Attenuation by Atmospheric Gases*, International Telecommunication Union, Geneva, Switzerland, 2013.
[35] *Receivers OEM628: Next Generation High Performance GNSS Receiver, Version 13*, Novatel, Inc., Calgary, Canada, 2015.
[36] E. R. Kursinski, "The GPS radio occultation concept: Theoretical performance and initial results," Ph.D. dissertation, Department of Geological and Planetary Sciences, California Inst. Technol., Pasadena, CA, USA, 1997.
[37] D. J. Jacob, *Introduction to Atmospheric Chemistry*. Princeton, NJ, USA: Princeton Univ. Press, 1999.
[38] B. Ahmed, "Accuracy and resolution of atmospheric profiles obtained from radio occultation measurements," Ph.D. dissertation, Department of Electrical Engineering, Stanford Univ., Stanford, CA, USA, 1998.
[39] *AMSU-A Level 1 Product Generation Specification*, EUMETSAT, Darmstadt, Germany, 2013.

Anne D. Marinan received the B.S. degree in aerospace engineering from the University of Michigan, Ann Arbor, MI, USA, in 2011, and the S.M. and Ph.D. degrees in aeronautics and astronautics from the Massachusetts Institute of Technology (MIT), Cambridge, CA, USA, in 2013 and 2016, respectively.

While with the Space Telecommunications, Astronomy, and Radiation Laboratory, MIT, she was also the Bus Systems and Power Engineer on the Microsized Microwave Atmospheric Satellite and performed power and GPS radio occultation simulations for the Microwave Radiometer Technology Acceleration Mission. She held a NASA Space Technology Research Fellowship from 2012 to 2016 while with MIT. She is currently in the Project Systems Engineering Section, Jet Propulsion Laboratory, Pasadena, CA, USA. Her research interests include adaptive optics and atmospheric modeling for CubeSat technology demonstration applications.

Dr. Marinan is a Member of the Society of Women Engineers and the SPIE.

Kerri L. Cahoy (S'00–M'08) received the B.S. degree in electrical engineering from Cornell University, Ithaca, NY, USA, in 2000, and the M.S. and Ph.D. degrees in electrical engineering, working with the Radio Science Team on Mars Global Surveyor, from Stanford University, Stanford, CA, USA, in 2002 and 2008, respectively.

In July 2011, she joined the Massachusetts Institute of Technology (MIT) Faculty, Cambridge, MA, USA, and leads the Space Telecommunications, Astronomy, and Radiation Laboratory. She is currently an Associate Professor in the Department of Aeronautics and Astronautics, MIT.

Rebecca L. Bishop received the B.S. degree in physics and B.S. degree in mathematics from the University of Idaho, Moscow, ID, USA, in 1996. She attended graduate school at the University of Texas at Dallas, Dallas, TX, USA, specializing in ionospheric physics. She received the Masters's degree in 1997 and the Ph.D. degree in 2001 from the University of Texas at Dallas, Dallas, TX.

She was a Postdoctoral with Clemson University, where her research interests include thermospheric dynamics and ionosphere/troposphere coupling via tropical storms and hurricanes. Since 2004, she has been with the Space Sciences Department, The Aerospace Corporation, El Segundo, CA, USA, as a Research Scientist. Her on-going research interests include characterizing the ionosphere/thermosphere using GPS radio occultation and other rocket-borne/satellite instrumentation, spacecraft charging effects on LEO satellites, and ionosphere/troposphere coupling.

Susan Seto Lui received the B.S.E.E. and M.S.E.E. degrees from the University of California, Los Angeles, CA, USA, in 1984 and 1986, respectively.

From 1980 to 2001, she was with the Hughes Space and Communications Group (HSC). While at HSC, she worked in the several different laboratories and business units. She designed digital GaAs IC's, designed and coordinated assembly of wafer and die level probe stations and test fixtures, and performed testing. She supported development of an S-level InP HEMT LNA with Hughes Research Laboratory and ran a full S-level MMIC packaging line as A Group Head. She was the REA for several units that required high-speed packaging and routing expertize, combining both digital and RF design principals. She has worked on Pico-Sat, MiRaTA (Cube-Sat Program), SSAEM, and supports a variety of PMP issues. In 2001, she joined The Aerospace Corporation, El Segundo, CA, where she led a multi-year effort to support the development of an optical communications system. Her current responsibilities include performing microwave measurements, modeling simulations for advanced receivers, transmitters, antennas, and related systems.

Ms. Lui is a Member of the TauBetaPi, the HKN, and the SWE.

James R. Bardeen received the B.S.E.E. degree from the University of Kansas, Lawrence, KS, USA, in 2001.

He was a Microwave Engineer with Vubiq, where he led the design of antennas and packaging for integrated 60-GHz radios. He is currently with The Aerospace Corporation, El Segundo, CA, USA, where has lead the development of free-space material characterization in the Antenna Systems Department. He has also designed and measured antennas for several small-satellite programs. While at The Aerospace Corporation, he has supported multiple programs including COSMIC-2 and GPS III. He holds four patents in integrated antennas in chip package technology and wireless communications.

Tamitha Mulligan received the B.S. degree in physics and physical chemistry, and the M.S. and Ph.D. degrees in geophysics and planetary physics from the University of California at Los Angeles (UCLA), Los Angeles, CA, USA, in 1996, 2000, and 2002, respectively.

She held a National Aeronautical and Space Administration Space Grant Fellowship from 1996 to 1999, while with UCLA. In 2004, she joined The Aerospace Corporation, Los Angeles, where she is currently a Research Scientist with the Space Materials Laboratory. Her professional activities have included the studies of solar transient phenomena, solar energetic particles, and galactic cosmic rays, and the subsequent effects that these phenomena have on the near-Earth space environment, including testing radiation effects on space materials and systems in the laboratory, studies of spacecraft charging, single-event effects, and geomagnetically induced currents.

William J. Blackwell (S'92–M'02–SM'07) received the B.E.E. degree in electrical engineering from the Georgia Institute of Technology, Atlanta, GA, USA, in 1994, and the S.M. and Sc.D. degrees in electrical engineering and computer science from the Massachusetts Institute of Technology (MIT), Cambridge, MA, USA, in 1995 and 2002, respectively.

He held a National Science Foundation Graduate Research Fellowship from 1994 to 1997. Since 2002, he has with MIT Lincoln Laboratory, Lexington, MA, where he is currently an Associate Leader of the Applied Space Systems Group. He is a Coauthor of *Neural Networks in Atmospheric Remote Sensing* (Norwood, MA, USA: Artech House, 2009) and *Microwave Radar and Radiometric Remote Sensing* (Ann Arbor, MI, USA: Univ. of Michigan Press, 2014). He has more than 100 publications related to atmospheric remote sensing. His primary research interests include atmospheric remote sensing, including the development and calibration of airborne and spaceborne microwave and hyperspectral infrared sensors, the retrieval of geophysical products from remote radiance measurements, and the application of electromagnetic, signal processing and estimation theory.

Dr. Blackwell is a Member of the Tau Beta Pi, the Eta Kappa Nu, the Phi Kappa Phi, the Sigma Xi, the American Meteorological Society, the American Geophysical Union, and the Commission F of the International Union of Radio Science. He is currently an Associate Editor of the IEEE TRANSACTIONS ON GEOSCIENCE AND REMOTE SENSING and the IEEE GRSS MAGAZINE. He is the Chair of the IEEE GRSS Remote Sensing Instruments and Technologies for Small Satellites Working Group, serves on the NASA Aqua Science Team and the National Academy of Sciences Committee on Radio Frequencies. He is the Principal Investigator on the NASA TROPICS Earth Venture Mission (2020 launch) and the Micro-Sized Microwave Atmospheric Satellite Missions (one launch in 2015 and two in 2017), and is Co-PI for the Microwave Radiometer Technology Acceleration CubeSat Mission (2017 launch). He was previously the Integrated Program Office Sensor Scientist for the Advanced Technology Microwave Sounder on the Suomi National Polar Partnership launched in 2011 and the Atmospheric Algorithm Development Team Leader for the NPOESS Microwave Imager/Sounder. He received the 2009 NOAA David Johnson Award for his work in neural network retrievals and microwave calibration. He received a poster award at the 12th Specialist Meeting on Microwave Radiometry and Remote Sensing of the Environment in March 2012 for "Design and Analysis of a Hyperspectral Microwave Receiver Subsystem" and received the IEEE Region 1 Managerial Excellence in an Engineering Organization Award "for outstanding leadership of the multidisciplinary technical team developing innovative future microwave remote sensing systems" in 2012.

Robert Vincent Leslie received the B.S degree from Boston University, Boston, MA, USA, and the M.S.a and Sc.D. degrees from the Massachusetts Institute of Technology, Cambridge, MA, USA, in 1998, 2000, and 2004, respectively, all in electrical engineering.

He is currently a Technical Staff with the Applied Space Systems Group, MIT Lincoln Laboratory, Lexington, MA, specializing in calibrating and testing passive microwave radiometers. He is the Calibration Lead for the Micro-Sized Microwave Atmospheric Satellite and the Microwave Radiometer Technology Acceleration CubeSats; the Principal Investigator for the JPSS microwave high-altitude sounder testbed; and the Project System Engineer for the NASA EVI-3 TROPICS mission. He is also a Member of the Advanced Technology Microwave Sounder Calibration/Validation team for S-NPP and JPSS.

Idahosa A. Osaretin (S'07–M'10) received the B.S. degree in electrical and computer engineering in 2006 and the M.S. and Ph.D. degrees in electrical engineering from the Ohio State University, Columbus, OH, USA in 2010 and 2011, respectively.

Since 2011, he has been with MIT Lincoln Laboratory, Lexington, MA, USA, where he is currently a Member of the Technical Staff. His current research interests include microwave radiometer design and analysis, compact reflector antenna design, compact and wideband horn feeds for reflector antennas, low-profile ultrawide band antenna design and analysis, microwave circuits, and electromagnetic wave propagation (radiation, scattering, and wave guiding) in complex environments.

Michael Shields received the M.S.E.E. degree from the University of Denver, Denver, CO, USA, in 1993, and the M.S. degree in applied mathematics from the University of Colorado, Boulder, CO, in 1985.

He is currently a Senior Staff Member with the Aerospace Sensor Technology Group, MIT Lincoln Laboratory, Lexington, MA, USA. His 40 year career in antennas and radar systems includes development of spacecraft telemetry antennas, phased arrays for ground, airborne and space applications, and reflector systems for both radar and passive sensing. These designs span the HF through submillimeter wave-frequency regimes. He has designed high-dynamic range receivers and small radar systems for various applications.